Self-calibration for two-dimensional stage using least squares solution

Xin Chen[1], Guoqing Ding[1,#], Satoru Takahashi[2] and Kiyoshi Takamasu[2]

1 Department of Instrument Science and Engineering, Shanghai Jiao Tong University, 800 Dongchuan Road, Shanghai 200240, China
2 Department of Precision Engineering, The University of Tokyo, 7-3-1 Hongo, Bunkyo-ku, Tokyo 1138656, Japan
Corresponding Author / E-mail: gqding@sjtu.edu.cn, TEL: +86-21-3420-7229, FAX: +86-21-3420-5372

KEYWORDS: Error Propagation, Least Squares Solution, Self-calibration, Two-dimensional Stage

Self-calibration is one of the main approaches to achieve a greater accuracy of the calibration in the field of the ultra-precise measurement. By measuring a rigid 2D artifact placed at different positions on a two-dimensional stage, it is possible to map the positioning errors of the stage in spite of the grid errors of the artifact. In this paper, an algorithm by use of least squares method is described to solve the problem of two-dimensional self-calibration. Exact reconstruction can be obtained in the absence of the random errors. Also, the error propagation characteristic of the random errors has been investigated. According to the simulation results, the error propagation ratio is less than 1 when the array size of the evaluated two-dimensional stage is less than 35 × 35. A fundamental experiment has been carried out on a vision measuring machine and the validity of the proposed self-calibration algorithm has been confirmed.

Manuscript received: January XX, 2011 / Accepted: January XX, 2011

NOMENCLATURE

n = one sided-point number of evaluated grid array
d = distance between the neighboring evaluated points
N_x, N_y = nominal coordinate values of evaluated points
M_x, M_y = measuring data defined in the machine coordinate system
S_x, S_y = stage errors defined in the stage coordinate system
A_x, A_y = grid errors of the 2D artifact defined in the artifact coordinate system
U_a, V_a = translation of the original points between the stage coordinate system and the artifact coordinate system
β_a = angle difference of the coordinate axises between the stage coordinate system and the artifact coordinate system
U_m, V_m = translation of the original points between the stage coordinate system and the machine coordinate system
β_m = angle difference of the coordinate axises between the stage coordinate system and the machine coordinate system

1. Introduction

With the fast development of integration and multi-functions of mechatronic system, there is an increasing demand for highly accurate geometrical measurement on mechanical and optical products[1]. For a precision measuring instrument, the two-dimensional stage with a large stroke is a key element to provide the lateral positioning with the accuracy of sub-micrometer or even nanometer[2]. But at this level, artifacts used as the references of the calibration, such as the linear scale and 2D ball plate, are far from perfect. Thus the calibration for the positioning errors of the stage (stage errors in the following) is a challenge in the field of ultra-precision measurement.

With respect to the absolute calibration method, which means that the accuracy of the calibration depends on the accuracy of the artifact, the self-calibration method exists[3]. One of the greatest features of the self-calibration is that the accuracy of the calibration does not depend on the accuracy of the artifact, just the repeatability of the stage itself. The original measuring process of the self-calibration is proposed by Raugh[4] for calibrating stage errors in electron beam lithography machines. But Raugh did not give a complete algorithm to reconstruct the stage errors. Until 1997, it is Ye[5] that proposed a valid algorithm based on Fourier transform method, which can achieve an error-free reconstruction in the absence of the random errors. Many applications, such as x-y stage of machine tool[6], out-of-plane errors of two-dimensional stages[7] and lens distortion of scanning probe microscope[8,9], have been performed by using the kind of the Fourier transform method. Furthermore, the two-dimensional algorithm is extended to the three-dimensional algorithm so that the three-dimensional self-calibration of coordinate measuring machine can be performed[10].

The existing algorithm based on the Fourier transform method is

very difficult for understanding. Also, the capability of the noise suppression is not so good. According to relative simulation results[5], the noise amplification factor is always larger than 1 and will increase along with the array size of the artifact. We recently developed an algorithm based on the least square solution. The modeling approach is much easier than existing algorithm for understanding. The paper is organized as follows: In Section 2, the principle of self-calibration will be introduced briefly. In Section 3, the model will be built by using matrix equations. The uncertainties associated with the reconstructed results are derived and the error propagation ratio is investigated. In Section 4, Computer simulations are performed with and without considering the random errors. In Section 5, fundamental experiments are carried out and the results are reported.

2. Principle of Self-calibration

The stage errors of a two-dimensional stage are calibrated by measuring a rigid two-dimensional artifact. As shown in Figure 1, the nominal form of the artifact should be a square grid array and the nominal pitch of neighboring grids is equal, although the actual grid errors of the artifact are unknown. The artifact is placed on the evaluated range of the stage and positioned laterally so that the x-y coordinate values for the center of each point of the artifact can be obtained. The same measurement process should be repeated for three different positions of the artifact at least, which are original position, 90 degree rotated position and one-pitch shift position. By use of a kind of algorithm, both the stage errors and the grid errors can be reconstructed from the three sets of measured data of the artifact. It should be pointed out that the misalignment errors among the different positions, which generally are of the same order as the stage errors, can be separated from measured data. Thus, there is no need to ensure an exact 90 degrees rotation or one-pitch shift of the artifact. The calibration accuracy mainly depends on the repeatability of the multi-position measurements.

3. Modeling and Least Squares Solution

The well-known algorithm to solve the problem of the two-dimensional self-calibration is using Fourier transform method developed by Ye[5]. In this section, a concise model of measurement process will be described and the least squares solution will be applied. The measured data, which are x-y coordinate values of grid points of the artifact, are based on the so-called global machine coordinate system. In order to calibrate the stage errors, other two coordinate systems (stage coordinate system and artifact coordinate system) can be defined.

3.1 Definition of Stage Coordinate System

Based on the machine coordinate system X_mOY_m, we can appoint a square grid array to be the evaluated range of the stage errors. Figure 2 shows the simplest case about 2×2 calibration positions which are connected by solid line. Note that it is not a point, just a tiny range for one position of the evaluated stage errors (4 hollow circles at the square vertexes shown in Figure 2). The vectors of the stage errors in each circle can be taken as the same size if we hypothesize the variation of the stage errors along the x or y axis is fairly slow. For the vectors ($S_{1\text{-}4}$) of the 4 calibration positions, we define a stage coordinate system X_sOY_s (dot line), in which the x and y components of the vectors can satisfy the following relationships[5]:

a) property of no translation,

$$\sum_{i=1}^{n\times n} S_x(i) = \sum_{i=1}^{n\times n} S_y(i) = 0 \ ; \tag{1}$$

b) property of no rotation,

$$\sum_{i=1}^{n\times n} \left[S_x(i)\cdot N_y(i) - S_y(i)\cdot N_x(i) \right] = 0 \ ; \tag{2}$$

c) property of no scale error,

$$\sum_{i=1}^{n\times n} \left[S_x(i)\cdot N_x(i) + S_y(i)\cdot N_y(i) \right] = 0 \ . \tag{3}$$

Here n denotes the number of one-dimensional points of two-dimensional stage errors. S_x and S_y denote the x and y components of the stage errors defined in the stage coordinate system. N_x and N_y denote the nominal coordinate values of the evaluated positions. We can also take U_m and V_m as the translation of the original points between the stage coordinate system and the machine coordinate system, take β_m as the angle difference of the coordinate axises between the stage coordinate system and the machine coordinate system. Since the stage coordinate system is adjusted finely with respect to the machine coordinate system, β_m can be taken as a tiny amount.

3.2 Definition of Artifact Coordinate System

The artifact is placed on the evaluated range of the stage. The nominal pitch of neighboring grids of the artifact should be equal to the interval between neighboring evaluated positions of the stage. Figure 3 shows the simplest case about 2×2 grid array which are displayed by solid circles. Unlike the vector of the stage errors, not

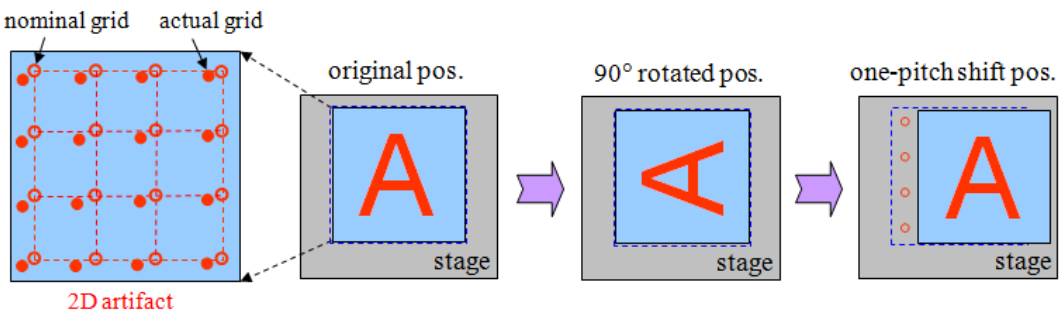

Fig. 1 Schematic diagram of self-calibration process for the two-dimensional stage

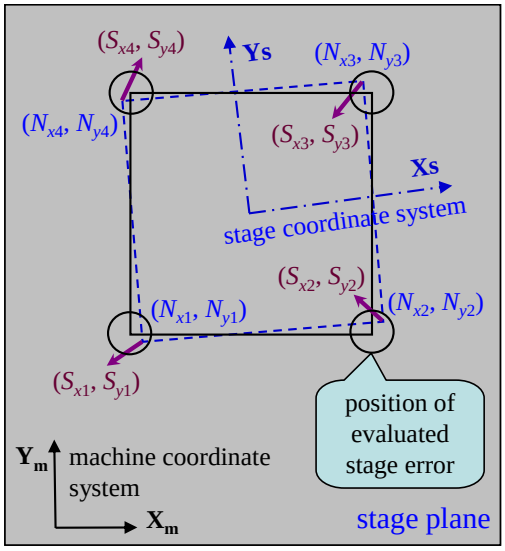

Fig. 2 Definition of stage coordinate system. $N_{1\text{-}4}$ denote the nominal coordinate values of the evaluated positions. $S_{1\text{-}4}$ denote the stage errors defined in the stage coordinate system

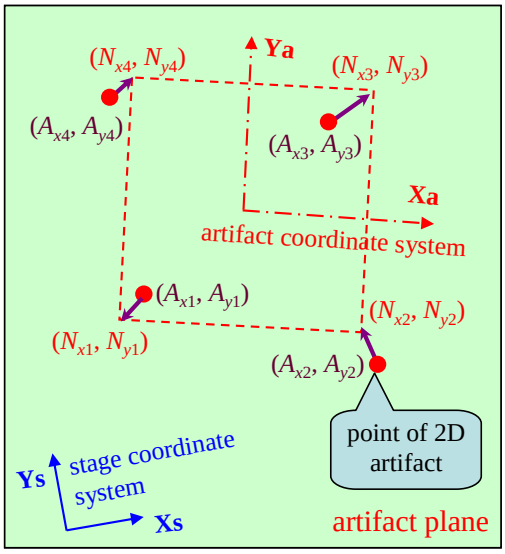

Fig. 3 Definition of artifact coordinate system. $N_{1\text{-}4}$ denote the nominal coordinate values of the grid points. $A_{1\text{-}4}$ denote the grid errors defined in the artifact coordinate system.

only the x and y components of the vectors of the grid errors, but also the vectors of the grid errors themselves are indeterminate unless a coordinate system is defined. As shown in Figure 3, we define an artifact coordinate system X_aOY_a (dot line), in which the x and y components of the grid errors can satisfy the following relationships[5]:

a) property of no translation,

$$\sum_{i=1}^{n\times n} A_x(i) = \sum_{i=1}^{n\times n} A_y(i) = 0 \ ; \tag{4}$$

b) property of no rotation,

$$\sum_{i=1}^{n\times n} \left[A_x(i)\cdot N_y(i) - A_y(i)\cdot N_x(i) \right] = 0 \ . \tag{5}$$

Here n denotes the number of one-dimensional points of 2D artifact. A_x and A_y denote the x and y components of the grid errors defined in the artifact coordinate system. N_x and N_y denote the nominal coordinate values of the grid points. Note that the property of no scale error is invalid in this case, because the artifact should be taken as a rigid body. We can also take U_a and V_a as the translation of the original points between the stage coordinate system and the artifact coordinate system, take β_a as the angle difference of the coordinate axises between the stage coordinate system and the artifact coordinate system. Since the artifact coordinate system is adjusted finely with respect to the stage coordinate system, β_a can be taken as a tiny amount.

3.3 Matrix Equation

The measured data M_x and M_y indicate the x-y coordinate values of grid points of the artifact in the machine coordinate system. We can obtain the corresponding vector expression in the stage coordinate system by using coordinate transform as follows:

$$\begin{aligned} \overrightarrow{\mathbf{Ms}} &= \begin{bmatrix} 1 & -\beta_m \\ \beta_m & 1 \end{bmatrix} \cdot \begin{bmatrix} M_x - U_m \\ M_y - V_m \end{bmatrix} - \begin{bmatrix} S_x \\ S_y \end{bmatrix} \\ &= \begin{bmatrix} M_x \\ M_y \end{bmatrix} - \begin{bmatrix} -N_y \cdot \beta_m \\ N_x \cdot \beta_m \end{bmatrix} - \begin{bmatrix} U_m \\ V_m \end{bmatrix} - \begin{bmatrix} S_x \\ S_y \end{bmatrix} \end{aligned} \ . \tag{6}$$

On the other hand, the corresponding vectors of the grid errors in the stage coordinate system can be expressed by using coordinate transform as follows:

$$\begin{aligned} \overrightarrow{\mathbf{As}} &= \begin{bmatrix} 1 & -\beta_a \\ \beta_a & 1 \end{bmatrix} \cdot \begin{bmatrix} A_x + N_x \\ A_y + N_y \end{bmatrix} + \begin{bmatrix} U_a \\ V_a \end{bmatrix} \\ &= \begin{bmatrix} A_x \\ A_y \end{bmatrix} + \begin{bmatrix} -N_y \cdot \beta_a \\ N_x \cdot \beta_a \end{bmatrix} + \begin{bmatrix} N_x + U_a \\ N_y + V_a \end{bmatrix} \end{aligned} \ . \tag{7}$$

Since Eq. (6) is equivalent to Eq. (7), we can obtain the following expression immediately:

$$\begin{aligned} &\begin{bmatrix} M_x \\ M_y \end{bmatrix} = \begin{bmatrix} S_x \\ S_y \end{bmatrix} + \begin{bmatrix} A_x \\ A_y \end{bmatrix} + \begin{bmatrix} -N_y \cdot \beta \\ N_x \cdot \beta \end{bmatrix} + \begin{bmatrix} U \\ V \end{bmatrix} \\ &\text{where} \quad \begin{bmatrix} \beta \\ U \\ V \end{bmatrix} = \begin{bmatrix} \beta_a + \beta_m \\ N_x + U_a + U_m \\ N_y + V_a + V_m \end{bmatrix} \end{aligned} \ . \tag{8}$$

According to Eq. (8), we can obtain a series of simultaneous equations easily with respect to original position, 90 degree rotated position and one-pitch shift position. By adding the constraint condition shown in Eq. (1-5), the observation equation can be expressed as follows:

$$\begin{aligned} &\mathbf{Y} = \mathbf{CX} \\ &\text{where } \mathbf{Y} = \left[\mathbf{M1_x}, \mathbf{M1_y}, \mathbf{M2_x}, \mathbf{M2_y}, \mathbf{M3_x}, \mathbf{M3_y}, 0,0,0,0,0,0,0 \right]^{\mathrm{T}} \\ &\qquad \mathbf{X} = \left[\mathbf{S_x}, \mathbf{S_y}, \mathbf{A_x}, \mathbf{A_y}, \beta_1, U_1, V_1, \beta_2, U_2, V_2, \beta_3, U_3, V_3 \right]^{\mathrm{T}} \end{aligned} \ . \tag{9}$$

Here $\mathbf{Y}$ denotes the column vector of the measured data at the three positions. Vector $\mathbf{M1_x}$, $\mathbf{M1_y}$, $\mathbf{M2_x}$, $\mathbf{M2_y}$ denote the M_x and M_y of all grid points at the original position and 90 degree rotated position respectively. Vector $\mathbf{M3_x}$, $\mathbf{M3_y}$ denote the M_x and M_y of all grid points except the last column of the artifact at the one-pitch shift position. $\mathbf{X}$ denotes the column vector of unknown parameters. Vector $\mathbf{S_x}$ and $\mathbf{S_y}$ denote the S_x and S_y of all evaluated positions. Vector $\mathbf{A_x}$ and $\mathbf{A_y}$ denote the A_x and A_y of all grid points. $U_{1\text{-}3}$, $V_{1\text{-}3}$ and $\beta_{1\text{-}3}$ denote the

corresponding U, V, β shown in Eq. (8) at the three positions respectively. **C** denotes the Jacobian matrix, the elements of which are determined by n, 0 and 1. The least squares solution of **X** can be obtained when the column rank of **C** is equal to the column size of **C**, also the row size of **C** is larger than the column size of **C**. The above conditions can be satisfied as long as $n \geq 2$. For instance, the row size of **C** is 287 and the column size is 205 when $n = 7$.

3.4 Error Propagation

In the least squares method, the uncertainty associated with the reconstructed stage errors and grid errors can be derived easily using the transmission matrix as follows[11]:

$$\mathbf{T_p} = (\mathbf{C}^{\mathrm{T}}\mathbf{T}^{-1}\mathbf{C})^{-1}. \tag{10}$$

Here **T** denotes the error matrix of the measured data, the elements of which can be determined by the standard deviation of the random errors of the measured data. For the 0 element among the last 7 elements of **Y**, we can appoint a very large number at the corresponding position of **T**. $\mathbf{T_p}$ denotes the error matrix of the parameters, the diagonal elements of which show the variances of the parameters. The expressions of the detailed elements for **T** and $\mathbf{T_p}$ are omitted here[11,12]. If we assume that the random errors of measured data at any position obey zero mean Gaussian distribution with no correlation, the error propagation ratio a can be calculated as follows:

$$a = \frac{1}{\sigma_m}\sqrt{\frac{1}{4\times n\times n}\sum_{i=1}^{4\times n\times n} u_x^2(i)}. \tag{11}$$

Here, σ_m denotes the standard deviation of the random errors. u_x denotes the uncertainties associated with S_x, S_y, A_x and A_y. In this case, the error propagation ratio depends on only one sided-point number of evaluated grid array. Figure 4 shows the relationship between one sided-point number of evaluated grid array and the error propagation ratio. Due to the restriction of the computer memory, we confirmed that the error propagation ratio is less than 1 when $n < 35$. This result is much better than the result by using Fourier transform method and indicates a good capability of the noise suppression by using the least squares solution.

4. Simulations

The computer simulations are performed to confirm the validity of the self-calibration algorithm. With many simulations, we confirm that the exact self-calibration can be obtained in the absence of the random errors of measured data. Next, an example of self-calibration on a 7×7 grid with interval of 1 mm is given when considering the random errors.

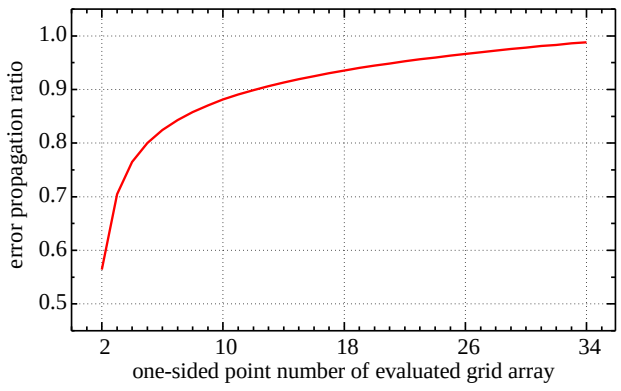

Fig. 4 Relationship between one sided-point number of evaluated array and the error propagation ratio

The stage errors (S_x, S_y) and the grid errors (A_x, A_y) are generated by using zero mean Gaussian distribution with standard deviation of 1 μm for both x and y components. $U_{1\text{-}3}$, $V_{1\text{-}3}$ and $\beta_{1\text{-}3}$ are chosen randomly for the three positions respectively. Note that $\beta_{1\text{-}3}$ should be tiny amounts. Vector **Y** is then constructed according to Eq. (8). Also, the random errors with standard deviation of 0.1 μm are added to vector **Y**. The reconstructed results (solid arrows) and the generated real values (dot arrows) of the stage errors are shown in Figure 5. The scale for the stage errors is 2 μm/div with respect to the scale for the actual grid interval with 1 mm/div. Figure 6 shows the residual (solid arrows) between the reconstructed results and the generated real values of the stage errors. The scale for the residual is 0.2 μm/div with respect to the scale for the actual grid interval with 1 mm/div. we can say that the residual owns the similar degree as the random errors

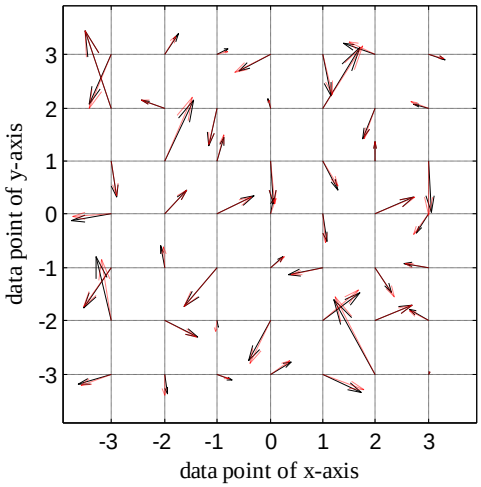

Fig. 5 Simulation results of self-calibration for stage errors on a 7×7 grid when considering the random errors. Solid arrows indicate the reconstructed results and dot arrows indicate the generated real values. The scale for the stage errors is 2 μm/div with respect to the scale for the actual grid interval with 1 mm/div.

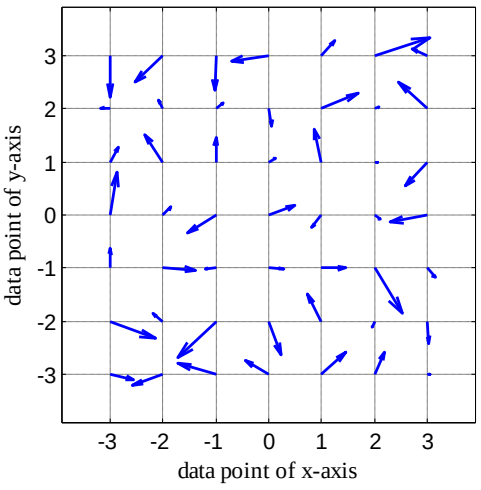

Fig. 6 Residual (solid arrows) between the reconstructed results and the generated real values of the stage errors. The scale for the residual is 0.2 μm/div with respect to the scale for the actual grid interval with 1 mm/div.

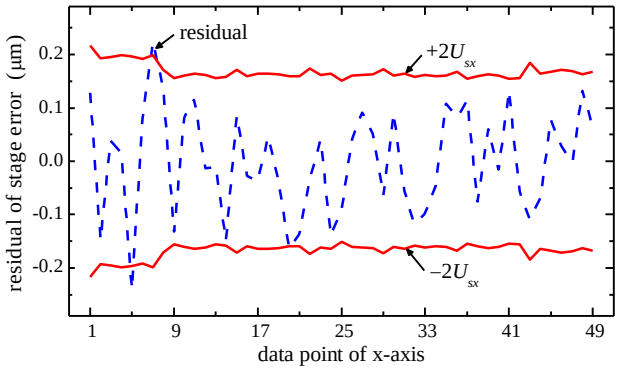

(a) x components of the stage errors

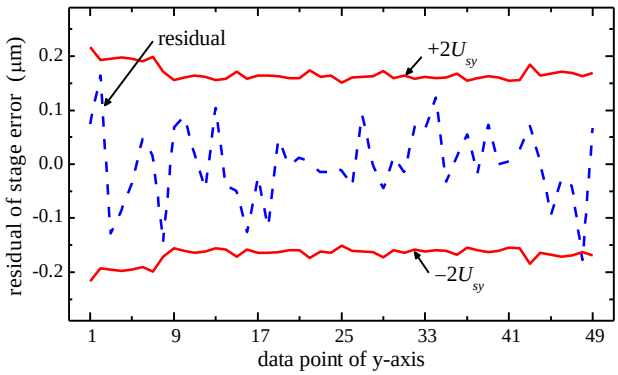

(b) y components of the stage errors

Fig. 7 Relationship between the theoretical uncertainties (solid line) associated with the stage errors and the residual (dot line).

in spite of the size of the stage errors or grid errors.

Figure 7 shows the relationship between the theoretical uncertainties (solid line, $\pm 2u_{sx}$ or $\pm 2u_{sy}$) associated with the stage errors and the residual (dot line) at each grid point. Figure 7(a) and (b) are the case of x and y components respectively. The uncertainties of first 7 points, which indicate the last column data not measured at the one-pitch shift position, are higher than the others. Because only 2 points (Figure 7(a)) and 1 point (Figure 7(b)) of the total 49 points of the residual are beyond the corresponding uncertainty curves, we confirm that the residual are covered by a 95% confidence interval.

5. Experiments

The fundamental experiments have been designed to calibrate the lens distortion of a vision measuring machine (resolution: 0.1 μm, accuracy: ±3 μm). A 2D grating with a nominal pitch of 136 μm, which is made by the laser etching on a silicon substrate, is used as the artifact. The artifact is placed just under the object lens of the vision measuring machine and is measured with several positions of rotation or shift. An automatic rotary stage is employed to make possible the rotation of the artifact. Figure 8 shows the photo of the experimental system. Only the centric 7×7 grid of the artifact is measured due to the FOV of the vision measuring machine.

Firstly the level of the random errors of the measured data from certain grid point is investigated. The result indicates that the root-mean-square of seven consecutive measurements is 0.8 μm. The measured data from the original position, 90 degree clockwise rotated position and one-pitch right-shift position are combined so that one

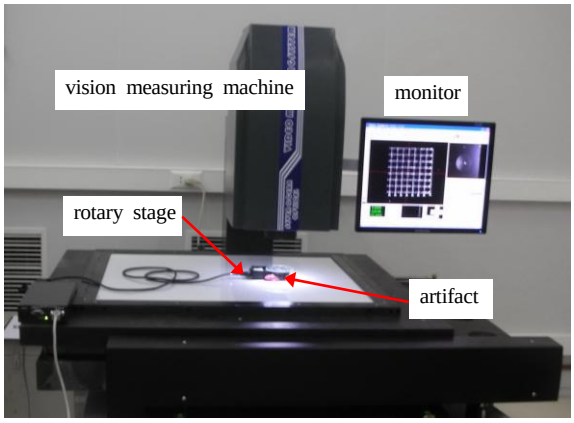

Fig. 8 Photo of experimental system for self-calibration

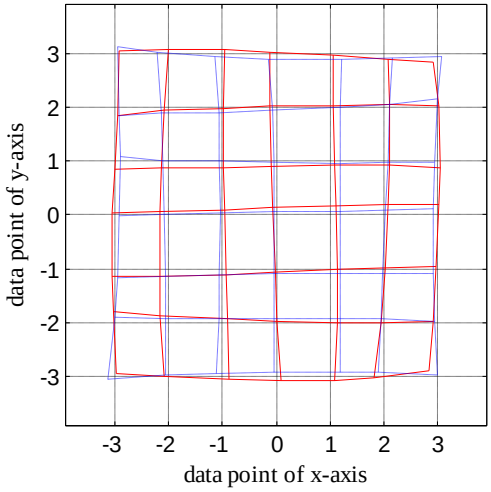

Fig. 9 Calibration results of the lens errors of the vision measuring machine on the 7×7 grid. Solid line is from result A and dot line is from result B. The scale for the lens errors is 10 μm/div with respect to the scale for the actual grid interval with 136 μm/div.

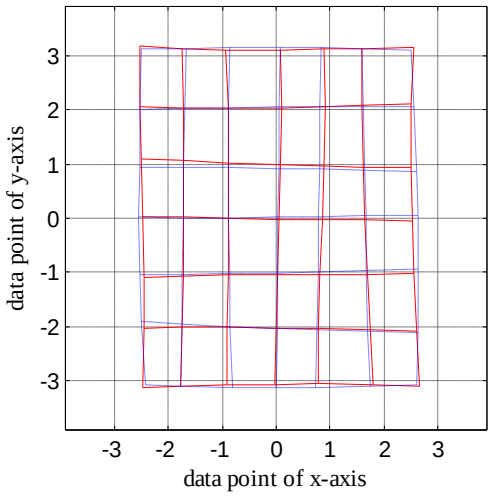

Fig. 10 Calibration results of the grid errors of the artifact on the 7×7 grid. Solid line is from result A and dot line is from result B. The scale for the grid errors is 20 μm/div with respect to the scale for the actual grid interval with 136 μm/div.

result (result A in the following) of self-calibration can be calculated. Also, the measured data from the original position, 90 degree anticlockwise rotated position and one-pitch left-shift position are combined so that the other result (result B in the following) of self-

calibration can be calculated. Figure 9 shows the lens errors of the vision measuring machine from result A (solid line) and result B (dot line) on the 7×7 grid. The scale for the lens errors is 10 μm/div with respect to the scale for the actual grid interval with 136 μm/div. The root-mean-square of the lens errors are 0.9 μm for both result A and result B. Figure 10 shows the grid errors of the artifact from result A (solid line) and result B (dot line) on the 7×7 grid. The scale for the lens errors is 20 μm/div with respect to the scale for the actual grid interval with 136 μm/div. Because the artifact we use is not a reference material for commercial use, the results indicate that the grid errors are rather large. Especially, the grid errors own a maximum of 11 μm at the x direction. On the other hand, the root-mean-squares of the differences between result A and result B are about 0.7 μm for both the lens errors and the grid errors. With respect to the random errors with the standard deviation of 0.8 μm as described above, the excellent characteristic for error propagation can be confirmed. As a result, we can say that the algorithm proposed can offer a valid self-calibration of the stage errors (here lens errors) in spite of the accuracy of the artifact[3-10].

6. Conclusions

In this paper, a self-calibration algorithm based on the least squares solution is proposed for two-dimensional stage. A concise model, which includes three different measurement positions of a 2D artifact, is developed to simplify the handling procedure with respect to the algorithm based on the Fourier transform method. When there are no random errors of measured data, the algorithms could provide an exact reconstruction of the stage errors in spite of the size of the grid errors of the artifact. When there are random errors of measured data, the good capability of noise suppression has been confirmed. The error propagation ratio is less than 1 when the array size of the evaluated two-dimensional stage is less than 35×35. A fundamental experiment has been carried out on a vision measuring machine. The lens errors of the vision measuring machine have been separated successfully from the grid errors of the artifact. The accuracy (1σ) of the calibration is about 0.7 μm, which is almost the same size of the random errors of the measured data.

ACKNOWLEDGEMENT

This research has been supported by the National Nature Science Foundation of China (No.50905116).

REFERENCES

1. Hansen, H. N., Carneiro, K., Haitjema, H. and De Chiffre, L., "Dimensional micro and nano metrology," Cirp Annals-Manufacturing Technology, Vol. 55, No. 2, pp. 721-743, 2006.
2. Holmes, M., Hocken, R. and Trumper, D., "The long-range scanning stage: a novel platform for scanned-probe microscopy," Precision Engineering-Journal of the International Societies for Precision Engineering and Nanotechnology, Vol. 24, No. 3, pp. 191-209, 2000.
3. Evans, C. J., Hocken, R. J. and Estler, W. T., "Self-calibration: reversal, redundancy, error separation, and 'absolute testing'," CIRP Annals - Manufacturing Technology, Vol. 45, No. 2, pp. 617-634, 1996.
4. Raugh, M. R., "Absolute Two-dimensional Sub-micron Metrology for Electron Beam Lithography," Precision Engineering, Vol. 7, No. 1, pp. 3-13, 1985.
5. Ye, J., Takac, M., Berglund, C. N., Owen, G. and Pease, R. F., "An exact algorithm for self-calibration of two-dimensional precision metrology stages," Precision Engineering-Journal of the American Society for Precision Engineering, Vol. 20, No. 1, pp. 16-32, 1997.
6. Takac, M. T., Ye, J., Raugh, M. R., Pease, R. F., Berglund, C. N. and Owen, G., "Obtaining a physical two-dimensional Cartesian reference," Journal of Vacuum Science & Technology B, Vol. 15, No. 6, pp. 2173-2176, 1997.
7. Yoo, S. B. and Kim, S. W., "Self-calibration algorithm for testing out-of-plane errors of two-dimensional profiling stages," International Journal of Machine Tools & Manufacture, Vol. 44, No. 7-8, pp. 767-774, 2004.
8. Klapetek, P., Necas, D., Campbellova, A., Yacoot, A. and Koenders, L., "Methods for determining and processing 3D errors and uncertainties for AFM data analysis," Measurement Science & Technology, Vol. 22, No. 2, pp. 2011.
9. Xu, M., Dziomba, T., Dai, G. and Koenders, L., "Self-calibration of scanning probe microscope: mapping the errors of the instrument," Measurement Science & Technology, Vol. 19, No. 2, pp. 2008.
10. Dang, Q. C., Yoo, S. and Kim, S. W., "Complete 3-D self-calibration of coordinate measuring machines," Cirp Annals-Manufacturing Technology, Vol. 55, No. 1, pp. 527-530, 2006.
11. Elster, C., Weingartner, I. and Schulz, M., "Coupled distance sensor systems for high-accuracy topography measurement: Accounting for scanning stage and systematic sensor errors," Precision Engineering, Vol. 30, No. 1, pp. 32-38, 2006.
12. Liu, S., Watanabe, K., Chen, X., Takahashi, S. and Takamasu, K., "Profile measurement of a wide-area resist surface using a multi-ball cantilever system," Precision Engineering, Vol. 33, No. 1, pp. 50-55, 2009.